



IFERC

Radiative divertor simulation and advanced divertor study for Demo tokamak reactor

**Nobuyuki Asakura, K. Hoshino, K. Shimizu
and Fusion Reactor Design group**

Aomori Research & Development Center, JAEA

**US Japan workshop on Fusion Power Plant
Related Advanced Technology
Kyoto University in Uji, Feb. 26-28, 2013**

Contents

- 1. Introduction:
power handling in DEMO divertor and SONIC simulation**
- 2. Impurity seeding and Long-leg for Demo power handling**
- 3. Effect of plasma diffusion on detachment**
- 4. Investigation of advanced divertor**
- 5. Summary and future work for DEMO divertor design**

1. Introduction: power handling in DEMO reactor

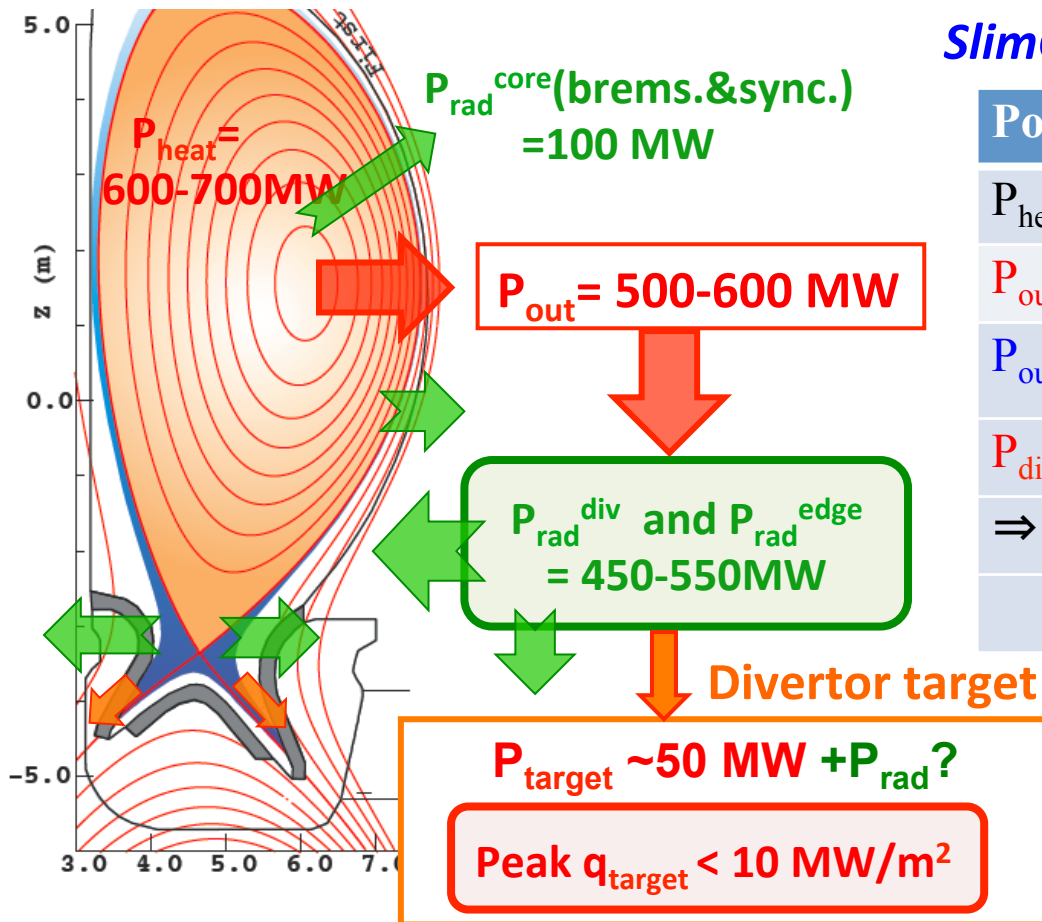
- Power handling is the most important issue for reactor design.

Demo reactor aiming $P_{el} = 1\text{GW} \Rightarrow P_{FP}$ of 3GW level [$P_{heat}(\alpha + \text{ad.}) = 600\text{-}700\text{ MW}$]

\Rightarrow Power exhaust to SOL (P_{out}) is 5-6 times larger.

\Rightarrow Radiation loss (P_{rad}) at the edge and divertor is required 10 times larger.

Energy (plasma, radiation, neutral) dissipation in the divertor to reduce peak q_{target}



SlimCS Demo tokamak for $P_{fus} = 2.95\text{ GW}$ [1]

Power handling		SlimCS	ITER
$P_{heat}(\alpha + \text{ad.})$	[MW]	650	150
$P_{out} = P_{heat} - P_{rad}^{core}$	[MW]	550	100
P_{out}/R_p	[MW/m]	100	16
$P_{div} (= P_{out} - P_{rad}^{div\&edge})$		< 50	~50
$\Rightarrow P_{rad}^{div\&edge}$	[MW]	~500	~50
$P_{rad}^{div\&edge}/P_{out}$		> 90%	~50%

Major radius : $R_p = 5.5\text{ m}$

Minor radius : $a_p = 2.1\text{ m}$

Plasma current : $I_p = 16.7\text{ MA}$

Toroidal field : $B_t = 6.0\text{ T}$

Plasma volume : $V_p = 941\text{ m}^3$

DEMO divertor design study for huge power handling

- Long divertor leg
- Increase *Wet area* with shallow target angle

Ref.4,5

Design parameters	ITER	SlimCS
f_{div}^{exp} (flux expansion)	4	3.7
L_{div} (outer leg length)	1.05m	1.73m
θ_{div} (target pol. angle)	24°	18°
A (wet area $\lambda_q^{mid}=5\text{mm}$)	1.9 m ²	3.0 m ²

⇒ increase radiation and recombination (dissipation) upstream of the target.

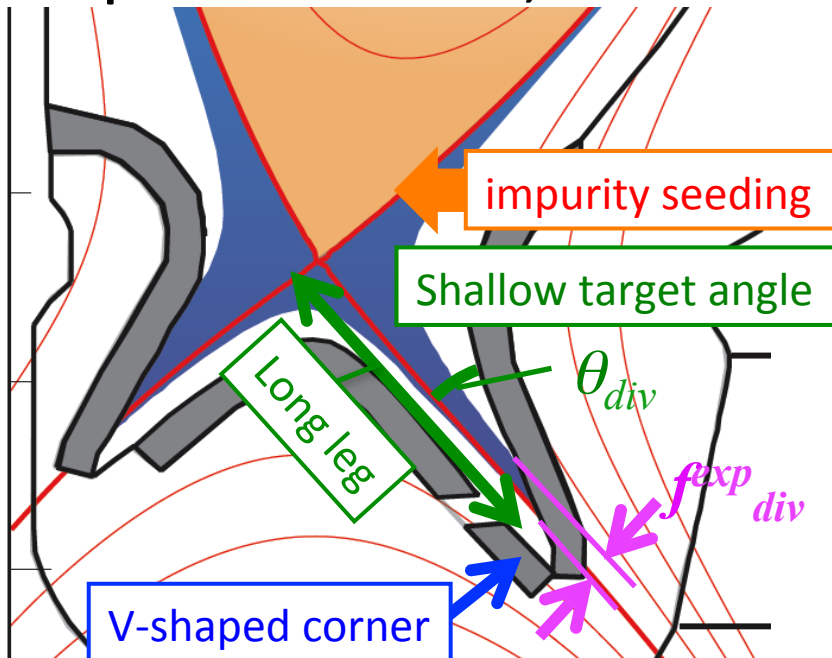
- **Impurity (Ar) seeding**

⇒ enhance edge and divertor radiation.

- **V-shaped corner**

⇒ further enhance neutral and impurity recycling near the strike-point.

SONIC code incl. MC impurity transport self-consistently simulates radiation distribution and plasma detachment, for the first time, under DEMO divertor condition.



Recent design study:

- Seeding impurity selection: radiation distribution and imp. screening

- Longer leg design (in geometry studies): further energy dissipation in divertor Ref.6

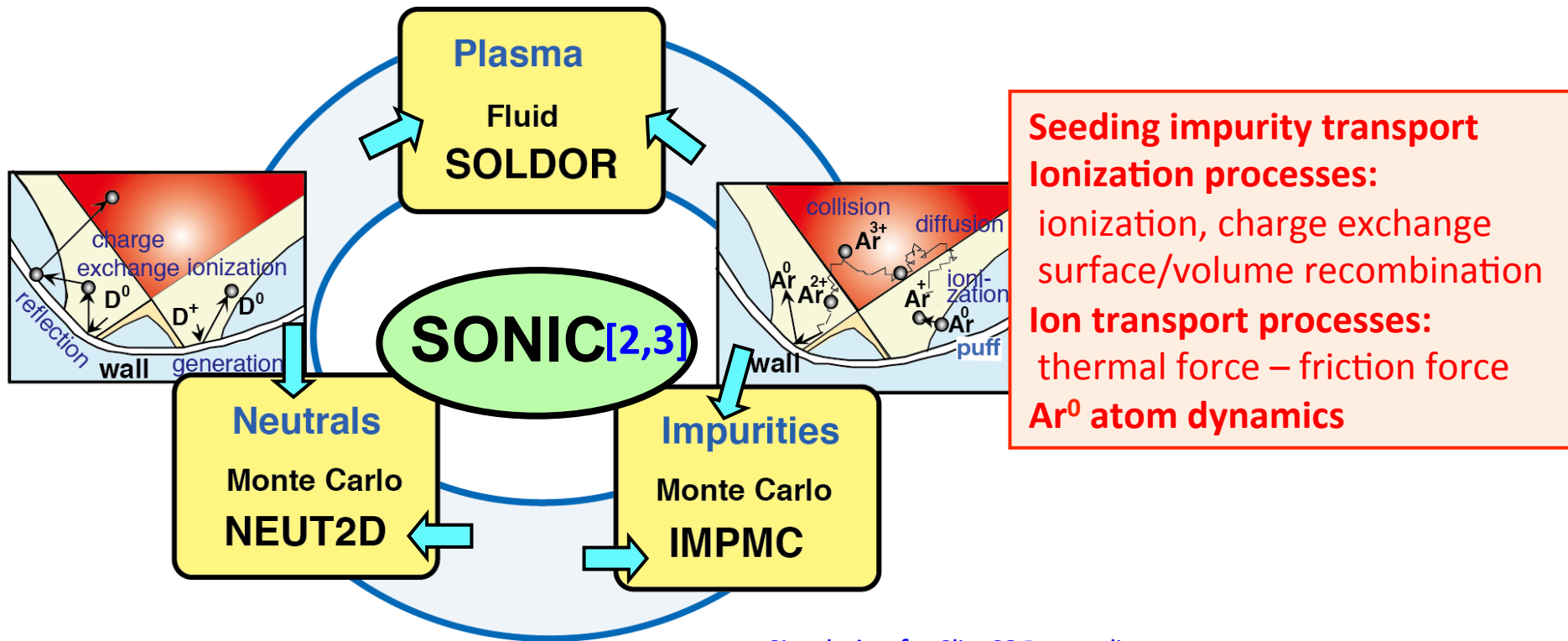
- Effects of plasma diffusion (transport studies): detachment and energy dissipation

SONIC: self-consistent coupling with impurity Monte Carlo has been developed for the divertor simulation

MC impurity simulation has advantage:

most impurity transport processes are incorporated in original formula such as

- Radiation & Recombination at multi-charge states
- Kinetic effect \Rightarrow Thermal force (temperature gradient force)



Seeding impurity transport
ionization processes:
ionization, charge exchange
surface/volume recombination
ion transport processes:
thermal force – friction force
Ar⁰ atom dynamics

Simulation for SlimCS Demo divertor:

[4] H. Kawashima, et al. Nucl. Fusion 49 (2009) 065007

[5] N. Asakura, et al. J. Plasma Fusion Res. SERIES 9 (2010) 136.

[6] K. Hoshino, et al. Contrib. Plasma Phys. 52 (2012) 550.

Development:

[2] K. Shimizu, et al., J. Nucl. Mater. 313-316 (2003) 1277

[3] H. Kawashima, et al. J. Plasma Fusion Res. 1 (2006) 31

Development of SONIC V2 for DEMO divertor simulation

Input parameters: $P_{\text{out}} = 500 \text{ MW}$, $n_e = 7 \times 10^{19} \text{ m}^{-3}$ ($r/a = 0.95$), $\chi_i = \chi_e = 1 \text{ m}^2 \text{ s}^{-1}$, $D = 0.3 \text{ m}^2 \text{ s}^{-1}$

(same diffusion coefficients for ITER simulation[7])

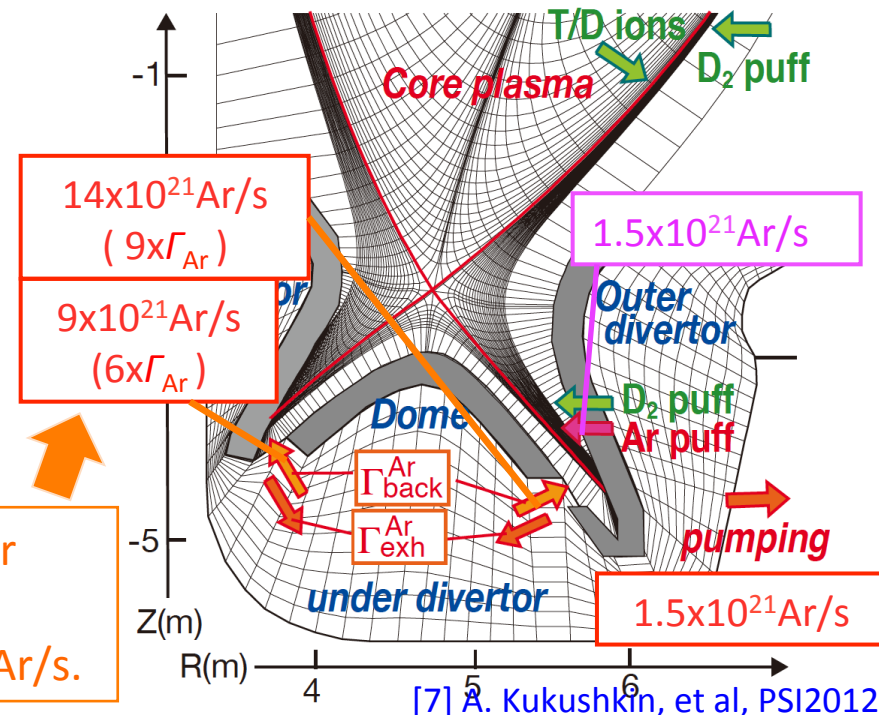
- Conversion of plasma solution was rather unstable/oscillating under Demo condition due to large q_{\parallel} and high T_e in SOL, and high flux and low T_{div} in divertor.



- Conversion became stable by recent improvements of SONIC simulation,

- (1) using distribution of impurity atom and particle balance under the divertor (exhaust route), which were calculated up to a steady-state condition (see below),
 \Rightarrow particle balance calculation was incorporated self-consistently in SONIC V3,
- (2) smoothing source terms near the target (by shorter time-step calculations) to reduce the MC noise,
- (3) correcting thermal force term for long mean-free-path (at high T_i), etc.

Self-consistent coupling solution of the fluid plasma, MC neutral and impurity was obtained "in steady-state".



Ar backflow from exhaust slots to the divertor plasma was handled as gas puff:
 $\Gamma_{\text{back}}^{\text{Ar}}(\text{in}) = 9 \times 10^{21}$ and $\Gamma_{\text{back}}^{\text{Ar}}(\text{out}) = 14 \times 10^{21} \text{ Ar/s}$.

2. Impurity seeding and Long-leg for Demo power handling

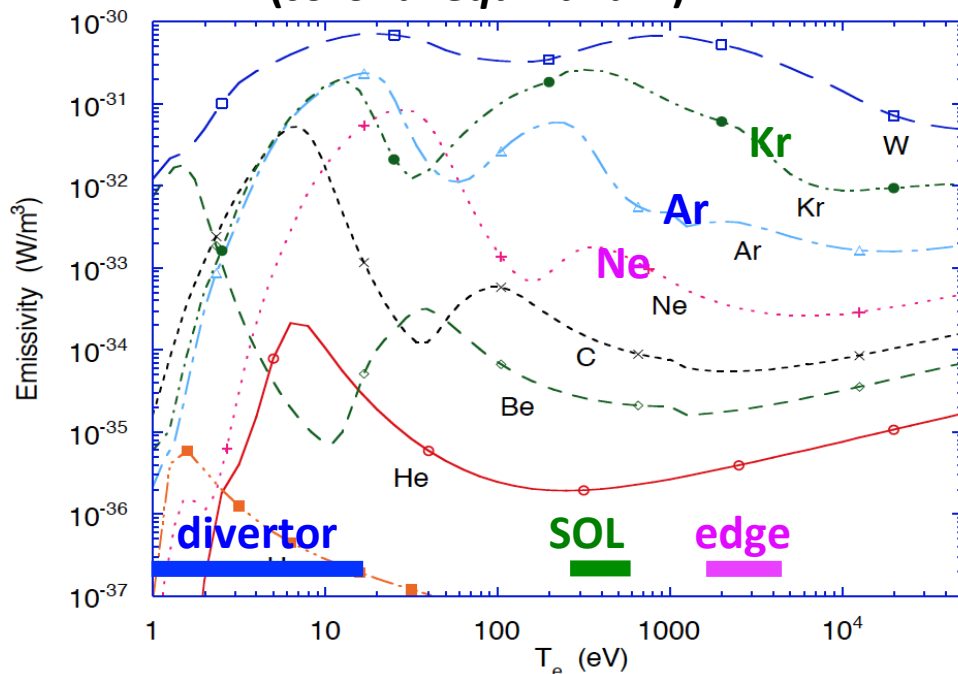
Under Demo edge condition, $T_e^{SOL} = 300\text{-}400\text{ eV}$, $T_e^{Edge} = \text{a few keV}$ are expected.

- Noble impurities radiate photon efficiently, enhancing at high T_e ($> 100\text{ eV}$) with Z .
 \Rightarrow appropriate radiators for Demo, which requires large radiation at SOL and edge.

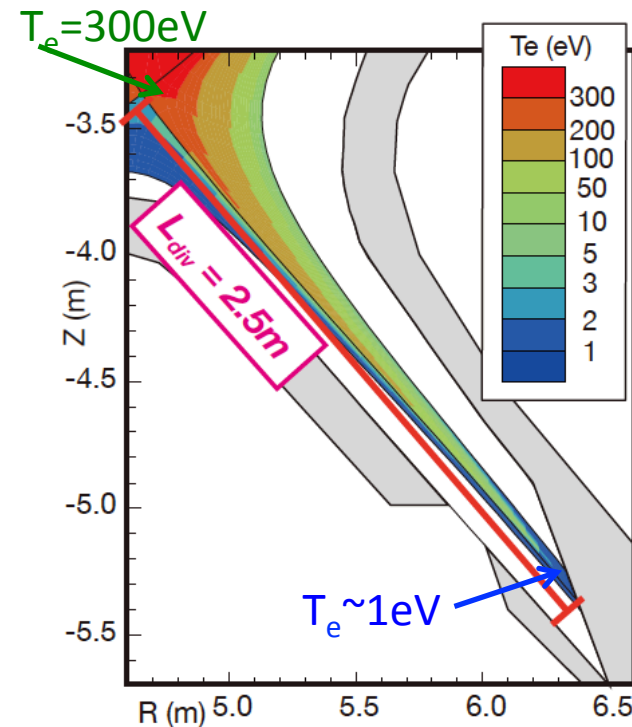
- Long leg divertor ($L_{//} = L_{div} B_{//} / B_p$) decreases $T_{div} \propto q_{//}^{10/7} / n_u^2 L_{//}^{4/7}$ (from 2-point model), and enhances particle & impurity recycling and produces detachment efficiently.

\Rightarrow appropriate length to produce full detachment and dissipation to reduce peak q_{target}

Radiation loss rate coefficients
(coronal equilibrium)



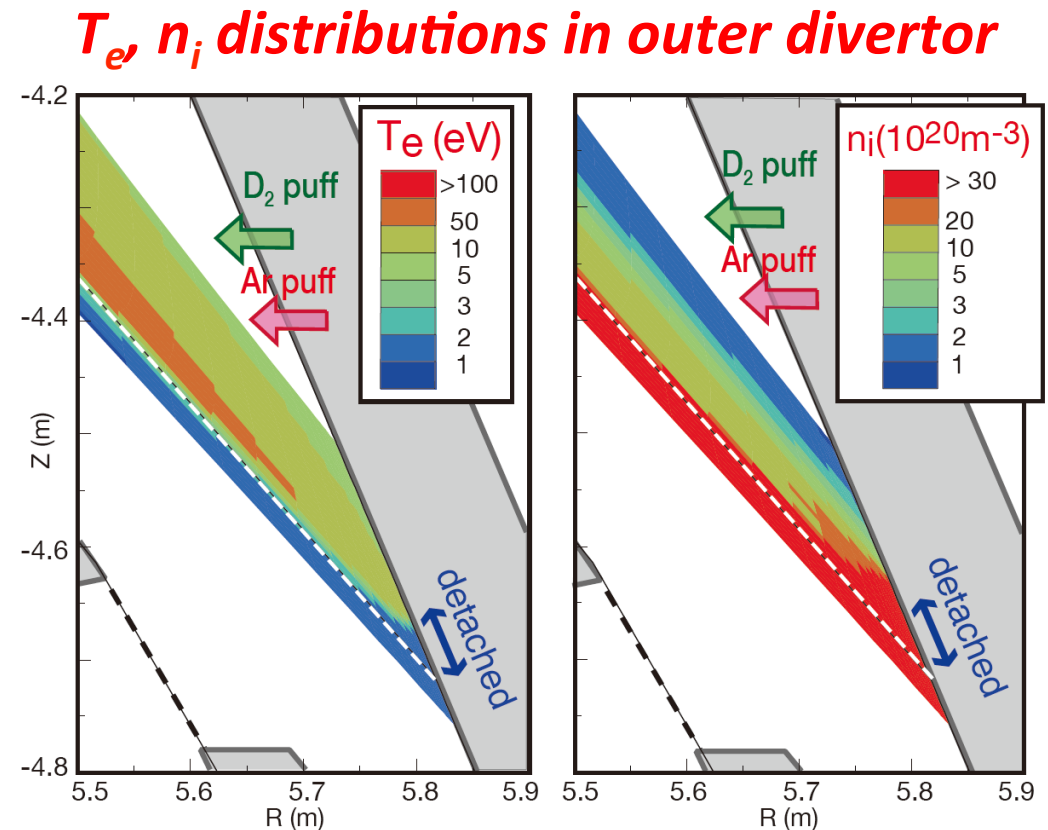
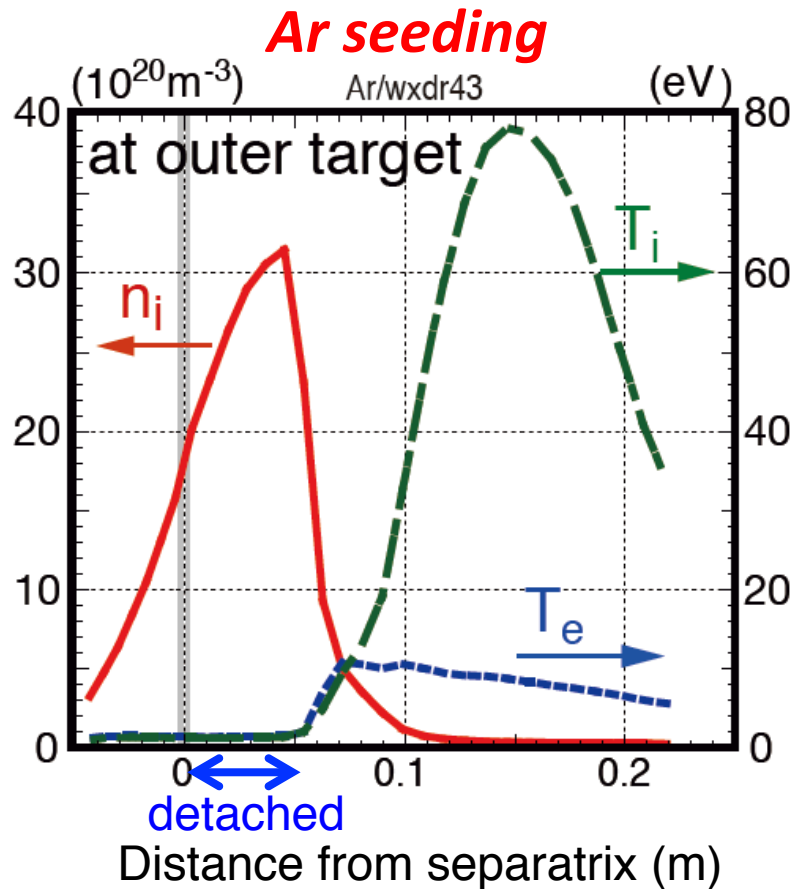
T_e distribution in Long leg divertor



2.1 Detachment in high radiative divertor

$P_{\text{rad}}^{\text{tot}}/P_{\text{out}}$ is increased to $\sim 92\%$ ($P_{\text{rad}}^{\text{tot}} = 460\text{MW}$) by Ar puff rate of $1.45 \times 10^{21} \text{ s}^{-1}$, radiation is distributed at edge and divertor: $P_{\text{rad}}^{\text{div}}/P_{\text{out}} = 61\%$, $P_{\text{rad}}^{\text{edge\&SOL}}/P_{\text{out}} = 31\%$.

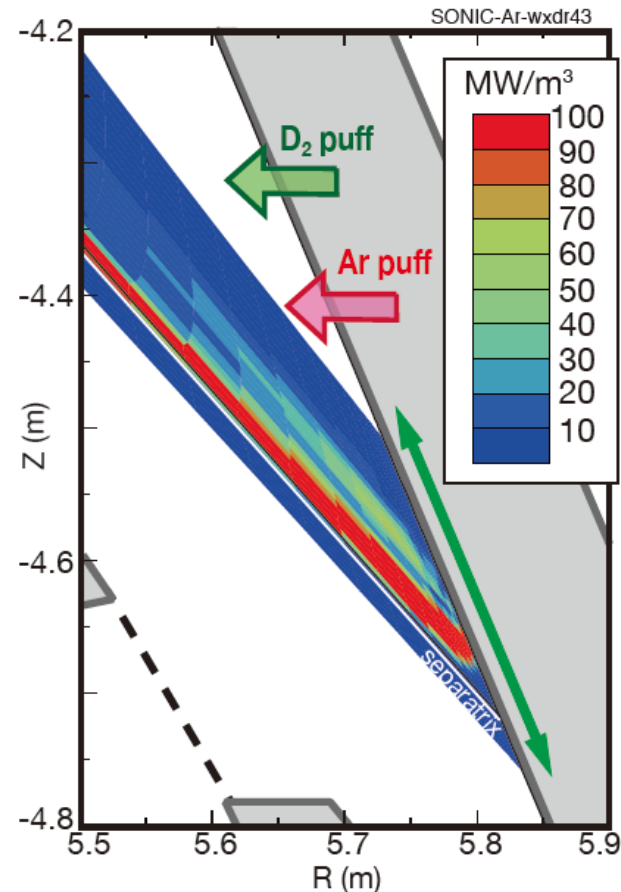
Partial detachment ($T_e < 1\text{-}2 \text{ eV}$) is seen *near the outer strike-point* ($< 5 \text{ cm}$), and Plasma is attached ($T_e = 10 \text{ eV}$, $T_i = 80 \text{ eV}$) *at outer flux surfaces* due to low density and low collisionality.



Power load profile at the outer target in detached divertor

- Plasma heat load (cond. + conv. + surface rec.) is reduced to $\sim 9 \text{ MWm}^{-2}$
surface recombination of low-temperature plasma contributes near the strike-point.
- Radiation power load is large ($3\text{-}5 \text{ MWm}^{-2}$) over a wide area in the divertor
 \Rightarrow peak heat load (q_{target}) is $\sim 16 \text{ MWm}^{-2}$ due to radiation source near above target.

Radiation distribution



- Total heat load on the target:

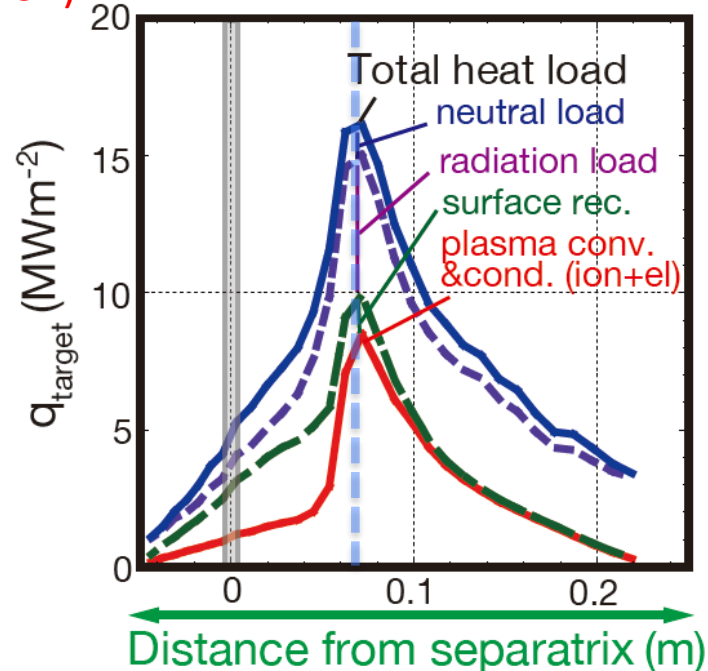
$$q_{\text{target}} = \underbrace{\gamma \cdot n_d \cdot C_{sd} \cdot T_d}_{\text{Plasma transport (conduction/convection of electron \& ion)}} + \underbrace{n_d \cdot C_{sd} \cdot E_{\text{ion}}}_{\text{Surface-recombination}} + \underbrace{f_1(P_{\text{rad}})}_{\text{radiation power load}} + \underbrace{f_2(1/2 m v_0^2 n_0 v_0)}_{\text{neutral load}}$$

Plasma transport
(conduction/convection
of electron & ion)

Surface-
recombination

radiation
power load

neutral
load



2.2 Radiation region and detachment extend for higher Z

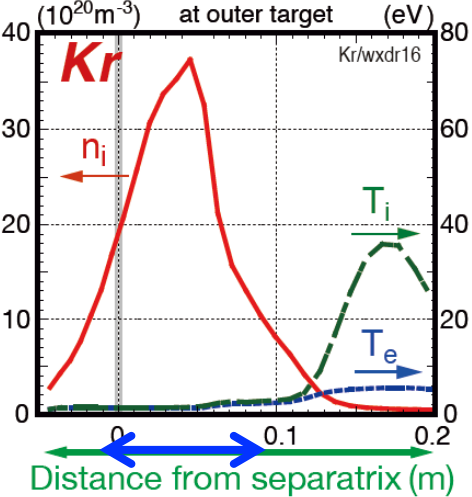
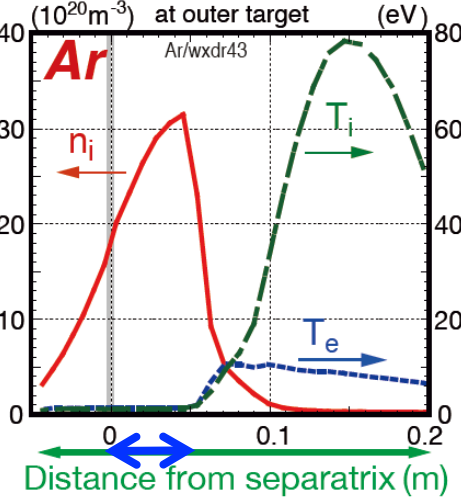
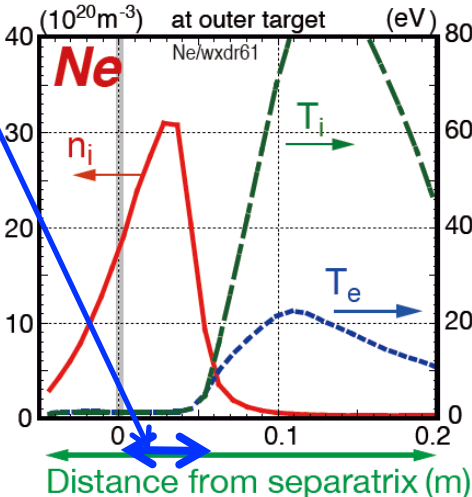
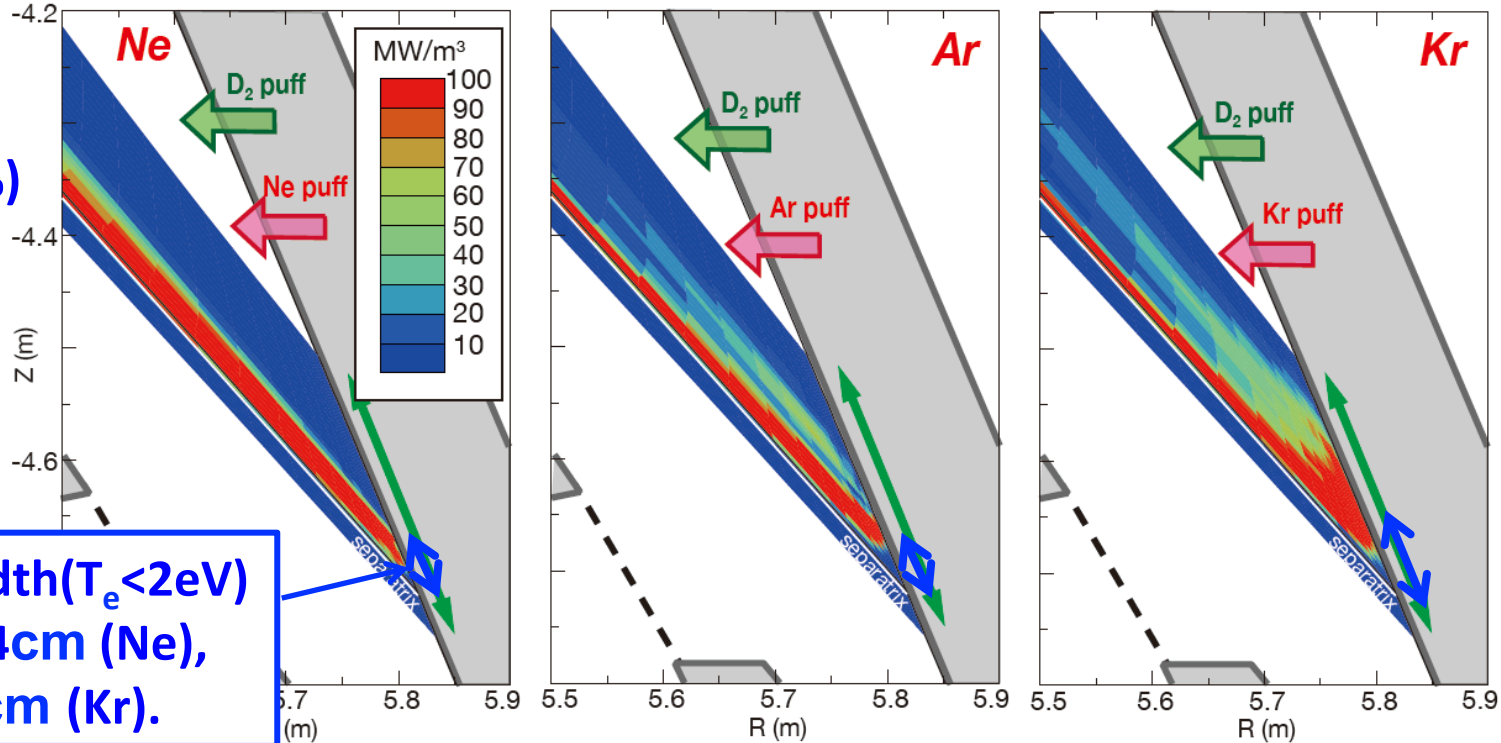
Influences of seeding impurity on radiation and target plasma are apparent for Kr.

All cases:

$P_{\text{rad}}^{\text{tot}} = 460\text{MW}$
 $(P_{\text{rad}}^{\text{tot}}/P_{\text{out}} \sim 92\%)$

puff	10^{21} atm/s
Ne	3.8
Ar	1.5
Kr	0.93

Detachment width ($T_e < 2\text{eV}$) increases from 4cm (Ne), 5cm (Ar) to 10cm (Kr).



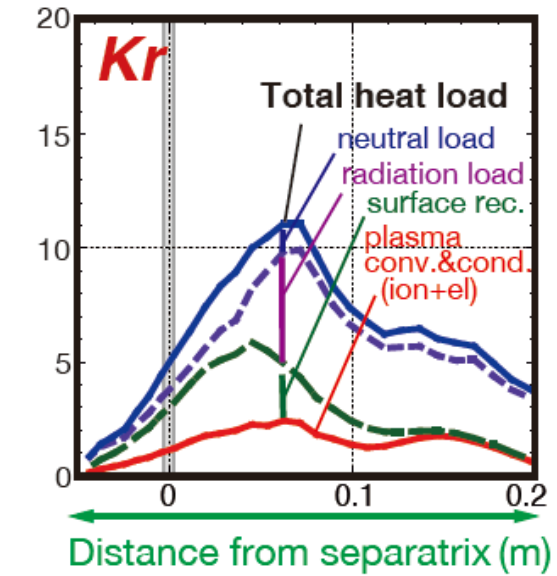
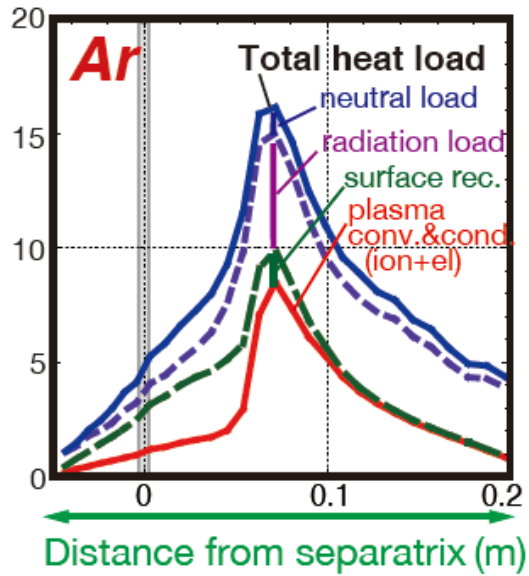
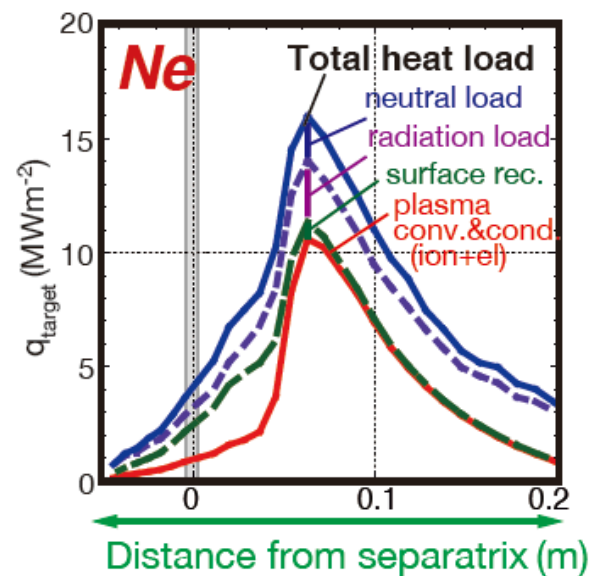
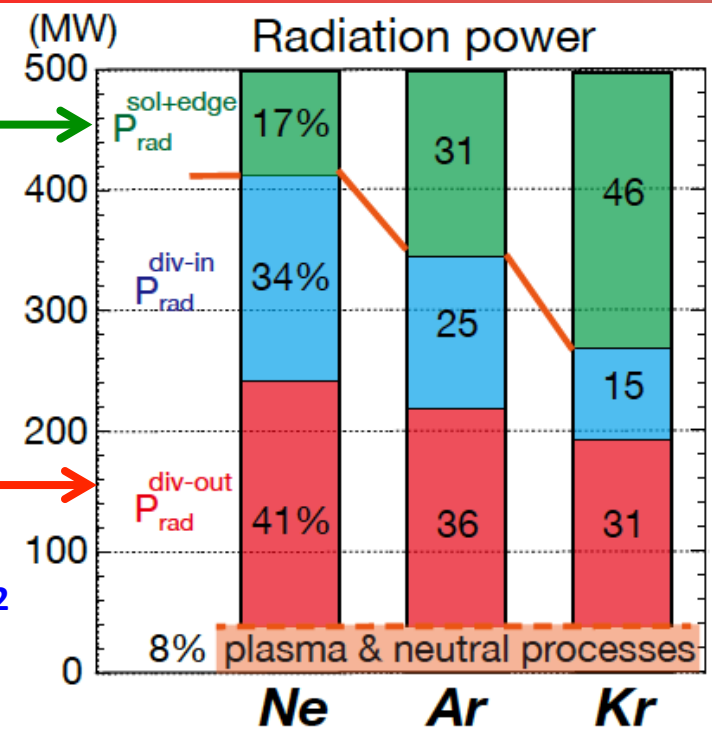
Detachment is efficient (high-Z) with decreasing power to divertor

For higher Z seeding, $P_{\text{rad}}^{\text{edge+sol}}$ increases from **86MW (Ne), 153MW (Ar), 229MW (Kr)**, where $P_{\text{rad}}^{\text{edge}} = 39\text{MW}(\text{Ne}), 53\text{MW}(\text{Ar}), 121\text{MW}(\text{Kr})$.

⇒ Peak heat load appears at the detach boundary, and it is reduced with *plasma heat load* (T_e & T_i).

$P_{\text{rad}}^{\text{div-OUT}}$ distribution changes from “near separatrix” (Ne) to “wide above target” (Kr), while $P_{\text{rad}}^{\text{div-OUT}}$ slightly decreases.

⇒ Radiation power load increases from ~2 MW/m² to 4-5 MW/m² over wide target area.



Impurity transport in SOL and edge

Impurity transport determines n_z distribution $\Rightarrow P_{\text{rad}}^{\text{div-OUT}}$, $P_{\text{rad}}^{\text{div-IN}}$ and $P_{\text{rad}}^{\text{div-SOL}}$, which are also determined by plasma transport (n_e , T_e , T_i , v_i) and rad.-process $L(T_e)$.

- Impurity screening for Ne, Ar, Kr is comparable

$$[(n_z/n_i)^{\text{div}}/(n_z/n_i)^{\text{SOL}}] = 1.5-2.$$

parallel force balance between *thermal force* ($F_{i\text{-therm}}$) and *friction force* (F_{fric}) is similar. [8]

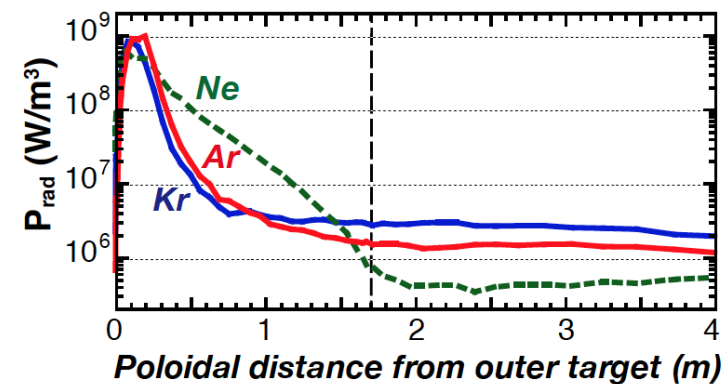
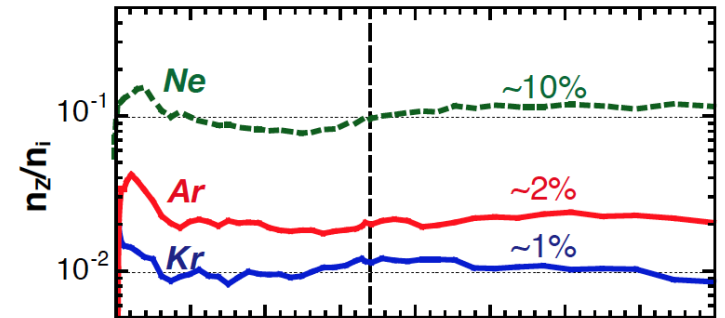
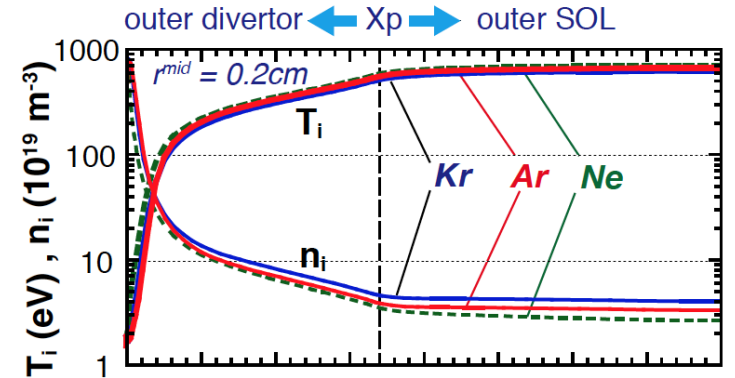
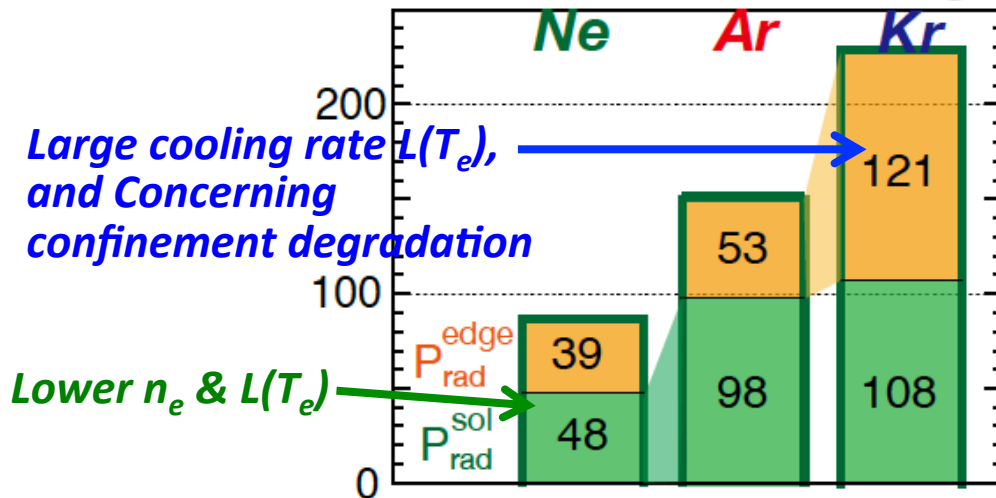
$$F_{i\text{-therm}} = \beta \nabla_{\parallel} T_i \sim 2.2 Z^2 \nabla_{\parallel} T_i \text{ [eVm}^{-1}, \text{eV]}$$

$$F_{\text{fric}} = (v_{\text{imp}} - v_i) \tau_{\text{imp}}^{-1} \sim 1.6 \times 10^3 Z^2 n_i M_{\parallel} T_i^{-1} \text{ [eVm}^{-1}, 10^{19} \text{m}^{-3}, \text{eV}]}$$

- Concentration $(n_z/n_i)^{\text{SOL}} \sim 0.1(\text{Ne}), 0.02(\text{Ar}), 0.01(\text{Kr})$, is determined by that in divertor.

Issue of the core plasma dilution remains for all.

(MW) Radiation at SOL & edge



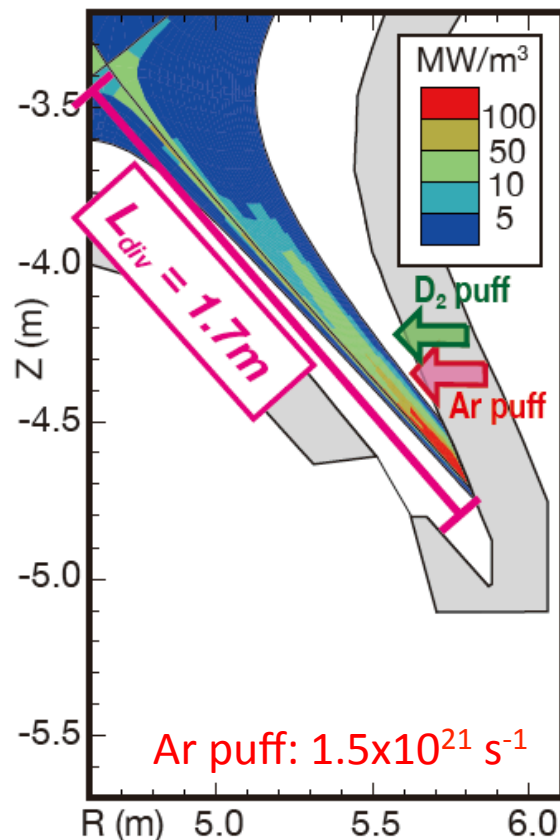
2.3 Effects of the Long-leg divertor

Divertor leg (L_{div}) is extended from 1.7 to 2.5 m, while flux expansion is reduced:

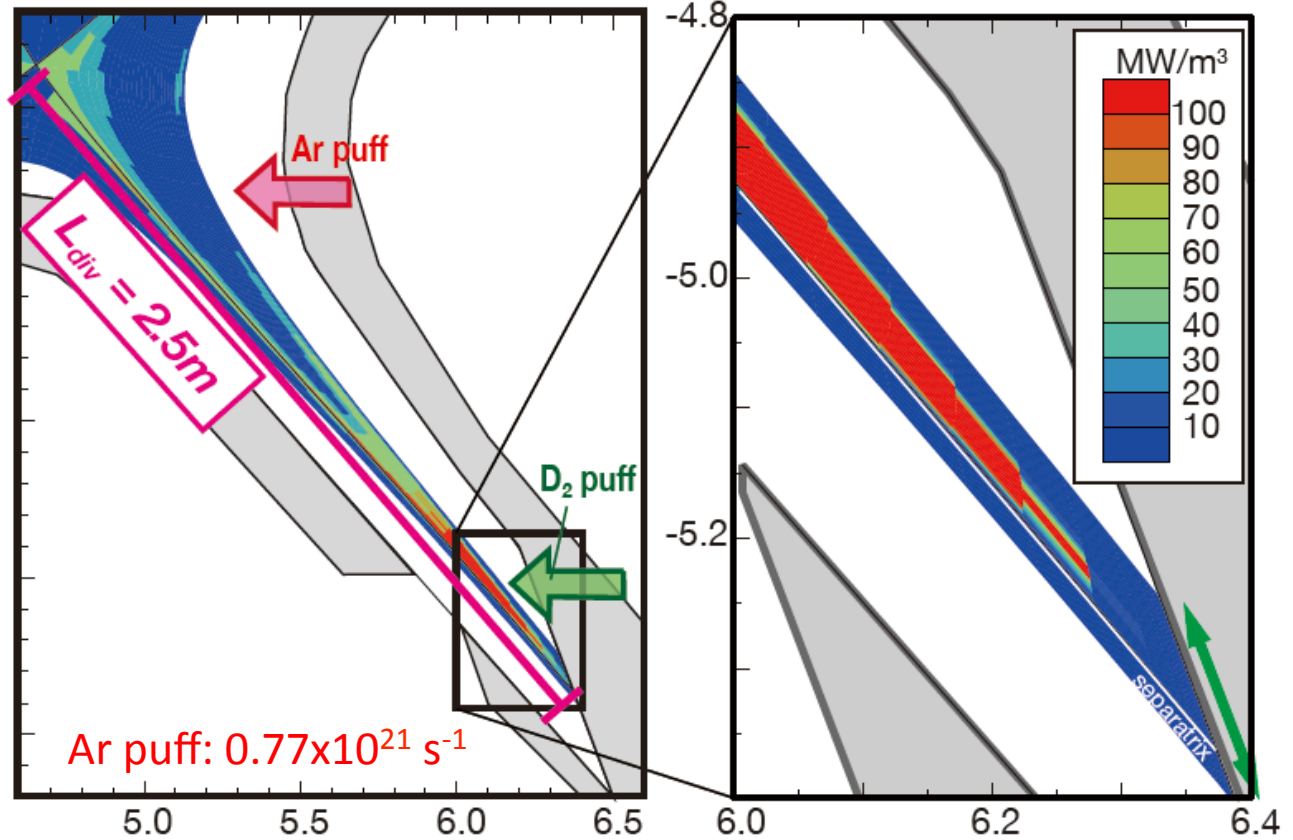
“Long leg divertor” decreases T_{div} and enhances particle & impurity recycling and produces detachment efficiently.

- Strong radiation region moves upstream, and still stays in the V-shaped corner \Rightarrow producing *full detachment*.

Radiation power density in Reference divertor

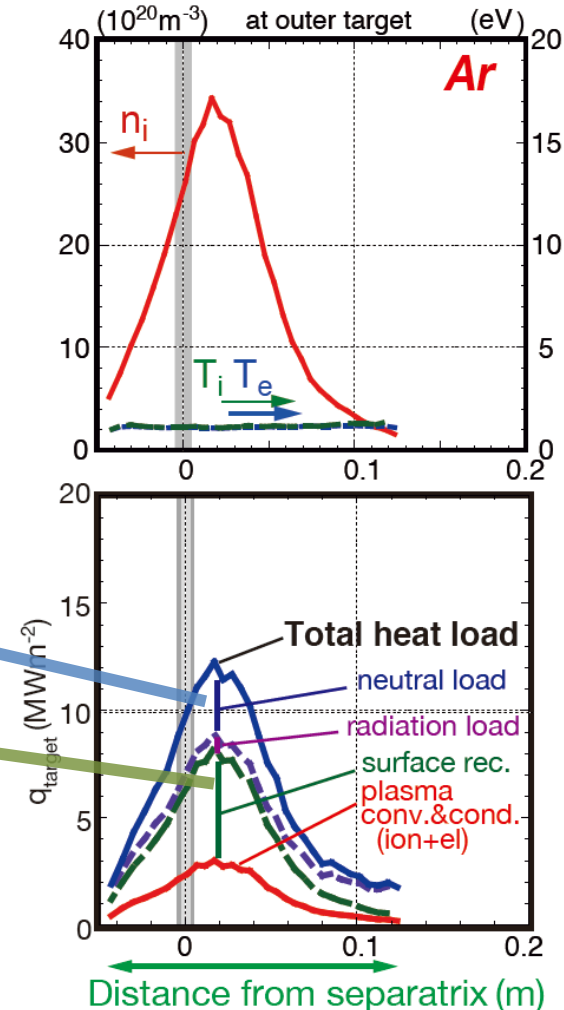
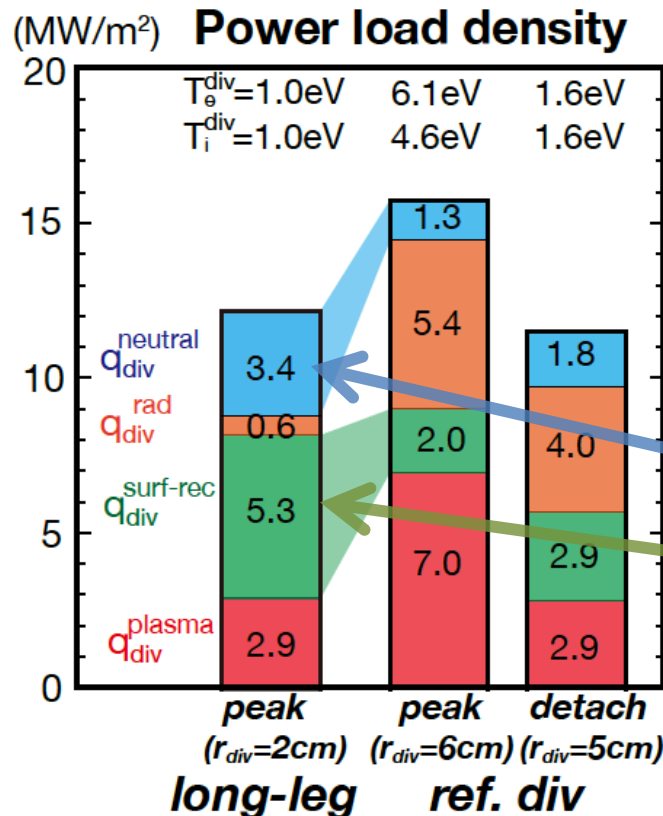
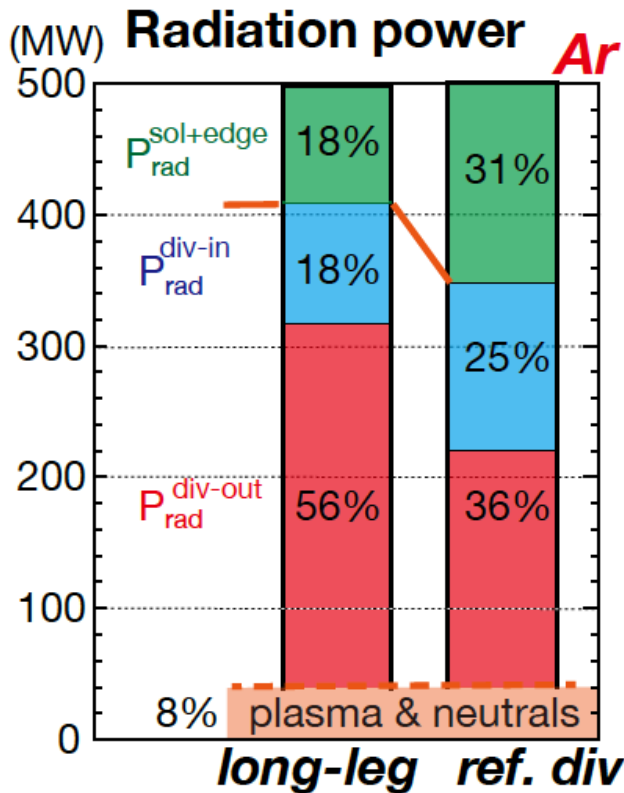


Radiation power density in Long-leg divertor



Effects of divertor length on radiation and detachment

- $P_{\text{rad}}^{\text{div-OUT}}$ largely increases in full detached divertor, while $P_{\text{rad}}^{\text{edge+SOL}}$ is reduced
 \Rightarrow radiation region is extended in the long-leg geometry
- Peak heat load decreases from 16 to 12 MWm⁻² in full detached divertor:
Radiation load as well as *plasma heat load* decrease significantly.
 \Rightarrow surface recombination due to low-temperature plasma and neutral flux by volume recombination increase, which may be caused by small flux expansion.



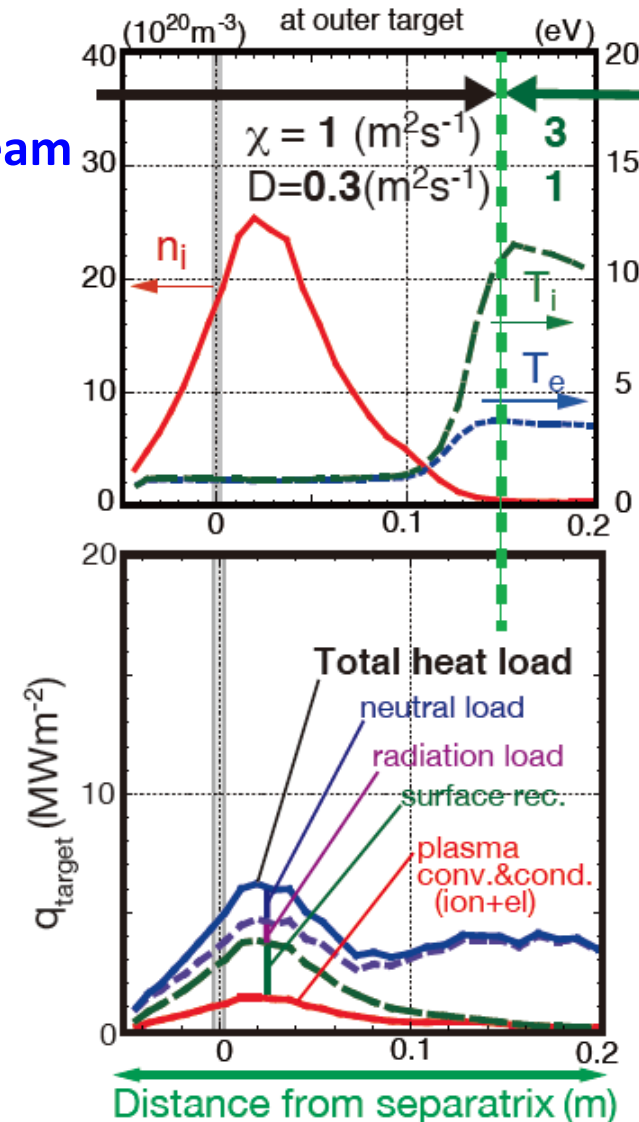
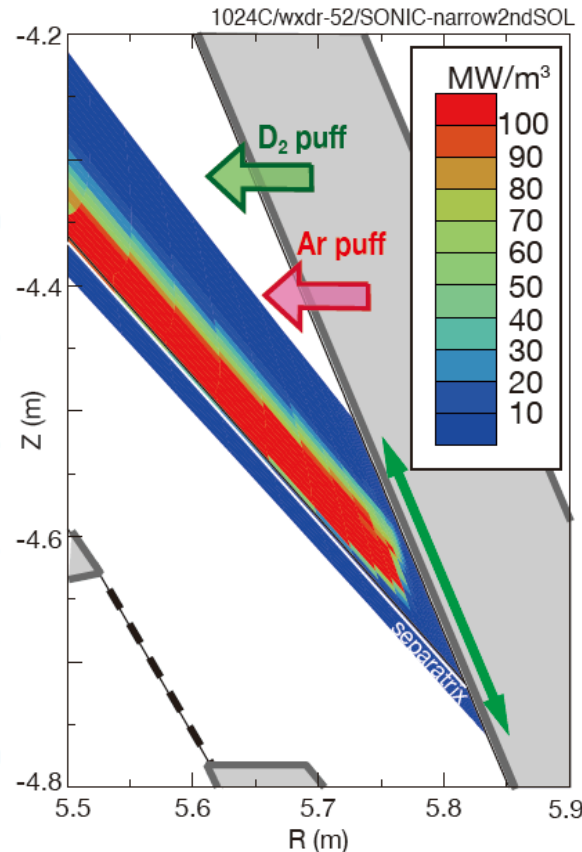
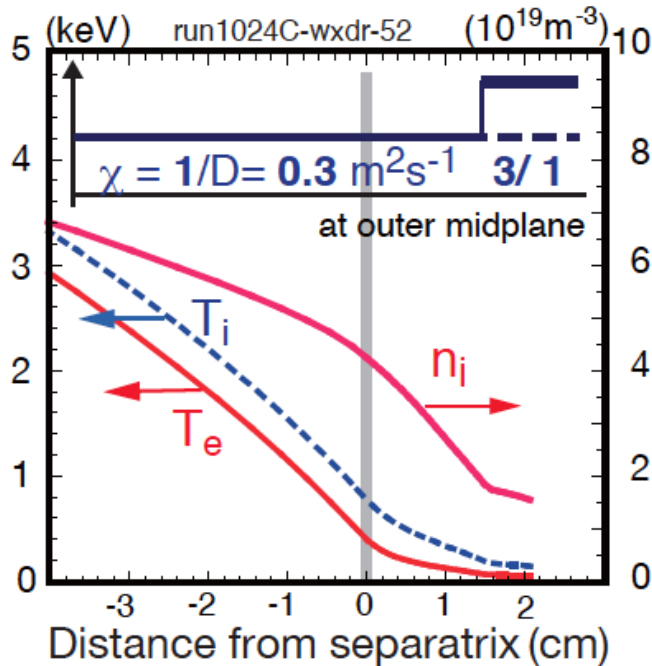
3. Effect of plasma diffusion on detachment

Diffusion coefficients change radially to simulate experiments such as “blob” :

Example-1: at the outer SOL ($r^{\text{mid}} \geq 1.5\text{cm}$: 15 cm at divertor), $\chi = 3 \text{ m}^2/\text{s}$ & $D = 1 \text{ m}^2/\text{s}$

- SOL plasma near the strike-point is influenced by **enhancement of diffusion in the outer SOL.**
- ⇒ T_i , T_e and n_e decrease, radiation region moves upstream
- ⇒ peak q_{target} is $\sim 7\text{MWm}^{-2}$

Plasma profile at midplane



Particle and energy dissipations enhance the detachment

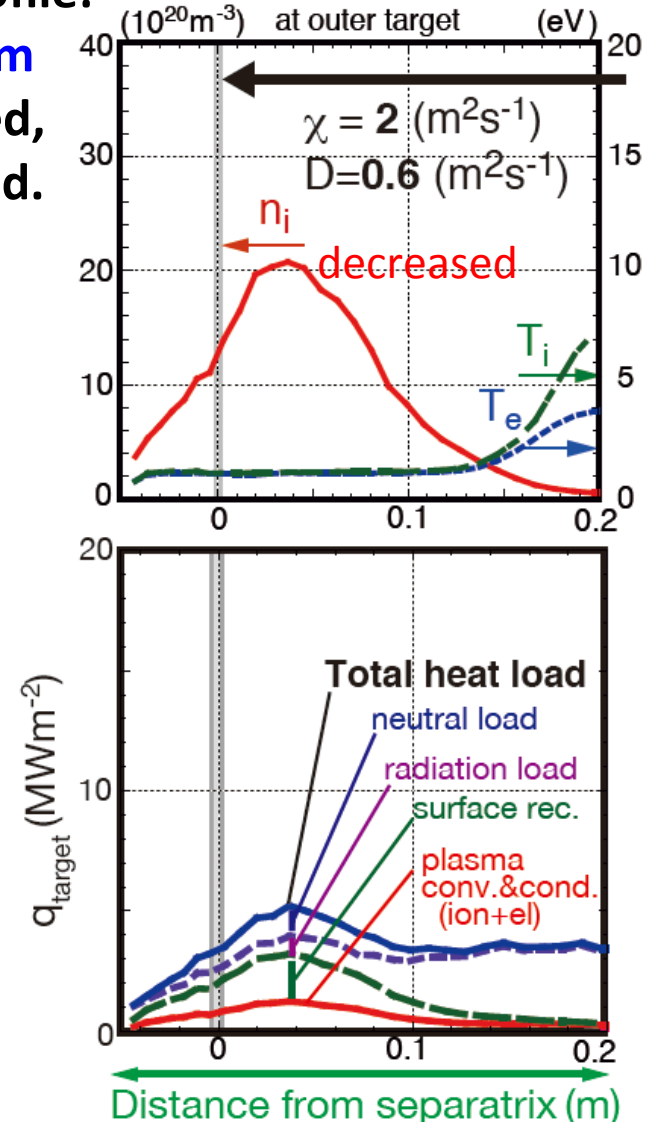
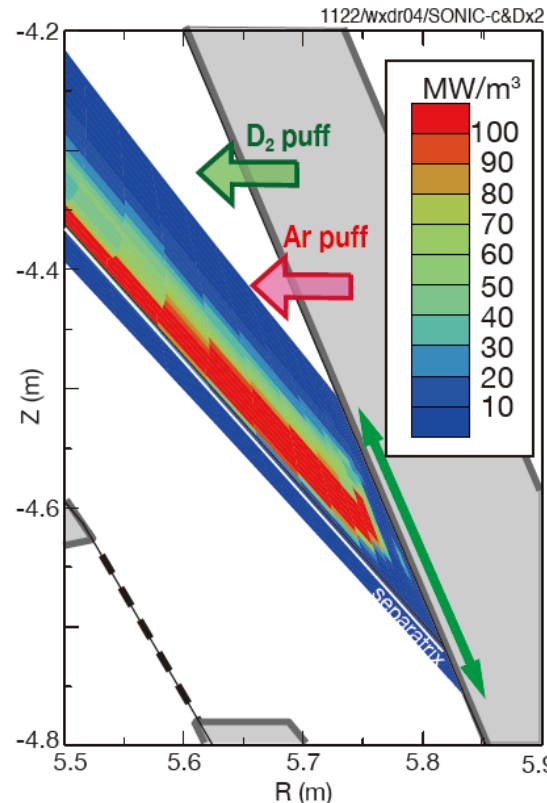
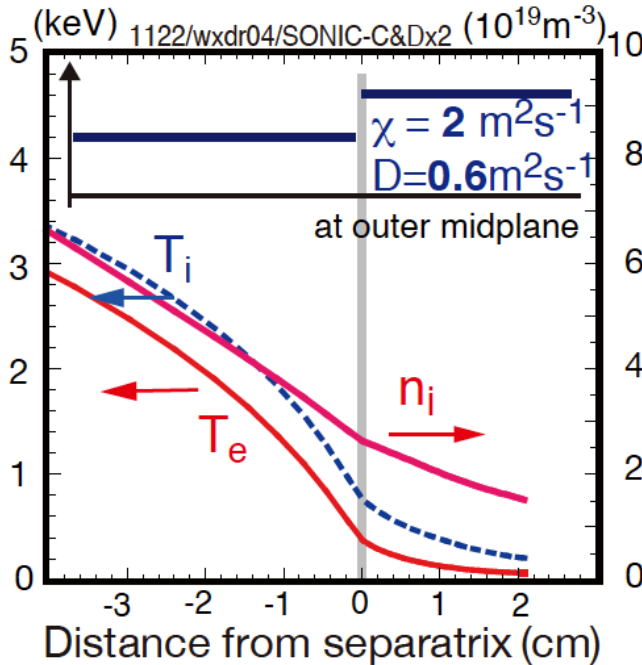
Example-2: enhancement of particle and energy dissipation in whole SOL & divertor

$\chi = 2 \text{ m}^2/\text{s}$ & $D = 0.6 \text{ m}^2/\text{s}$ (bouble) $\Rightarrow \lambda_q^{\text{SOL}}$ is increased only from 2.2 to 2.7mm.

- Diffusion largely affects detachment and heat load profile:

T_i , T_e and n_e decrease, radiation region moves upstream
 \Rightarrow peak q_{target} is $\sim 5 \text{ MWm}^{-2}$: full detachment is produced,
 surf. recombination and neutral flux are also reduced.

Plasma profile at midplane



4. Investigation of “advanced divertor” as new options

Advanced divertors “*Super-X divertor*” and “*Snowflake divertor*” have advantage to increase both **connection length ($L_{//}$)** and **wet area (A_{wet})** \Rightarrow **Reduction in peak q_{target}**

$$q_{target} = P_{div}/A_{wet}, \text{ where } A_{wet} = f^{exp}_{div} (R_{div}/R_{mid}) A_{mid}/\sin\theta_{div}, f^{exp}_{div} \approx [B_p/B]_{div}/[B_p/B]_{mid}$$

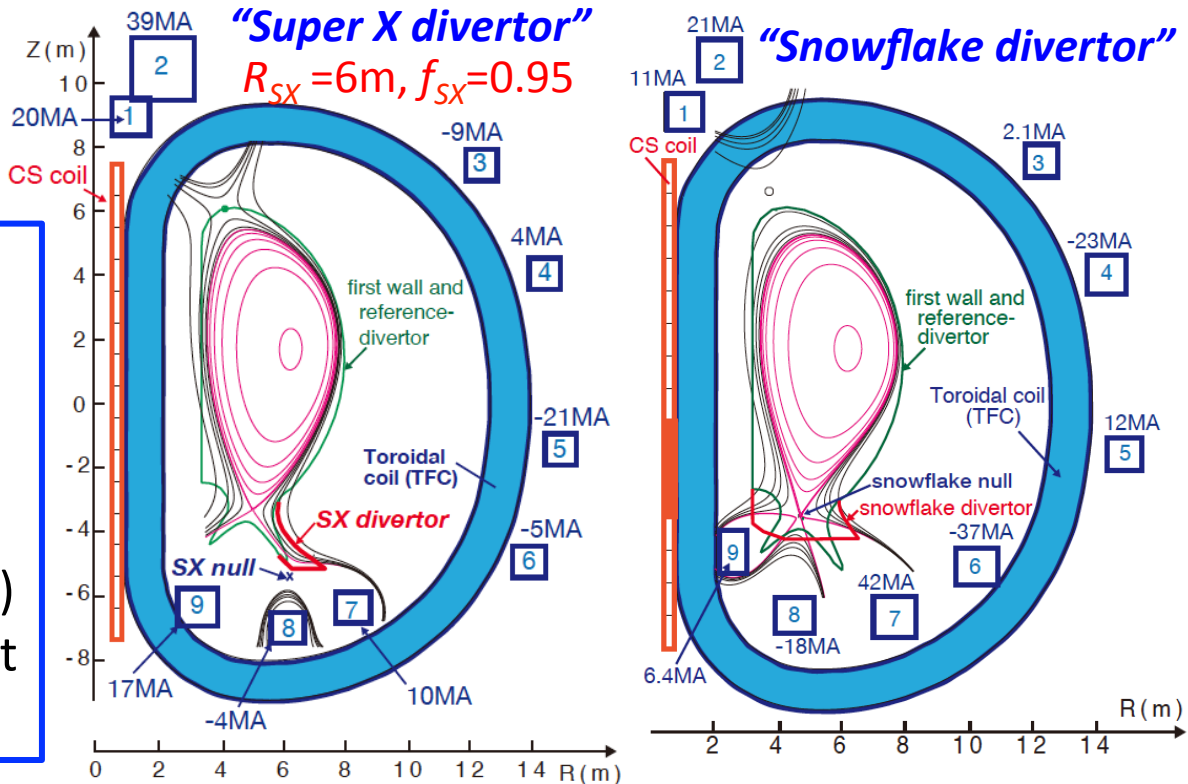
“*Super X divertor*”: f^{exp} and $L_{//}$ are increased from the divertor null to SX null, introducing **SX-null: R_{SX}** , and **Flux ratio of SX-null: $f_{SX} = (\Psi_{SXD} - \Psi_{mag})/(\Psi_s - \Psi_{mag})$**

“*Snowflake divertor*”: large f^{exp} and long $L_{//}$ are produced near SF null \Rightarrow Enhancement of P_{rad} and reduction of peak $q_{//}$ are expected in a compact divertor.

- Divertor coil location (inside or outside TFC) and target location are determined.

Restrictions of the poloidal coil location for Demo design:

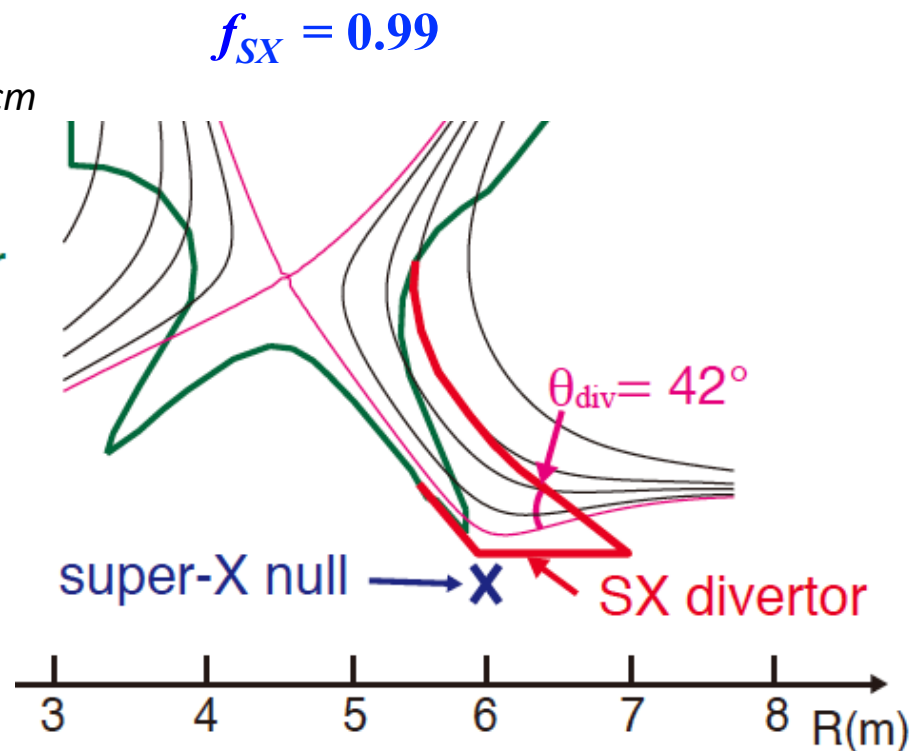
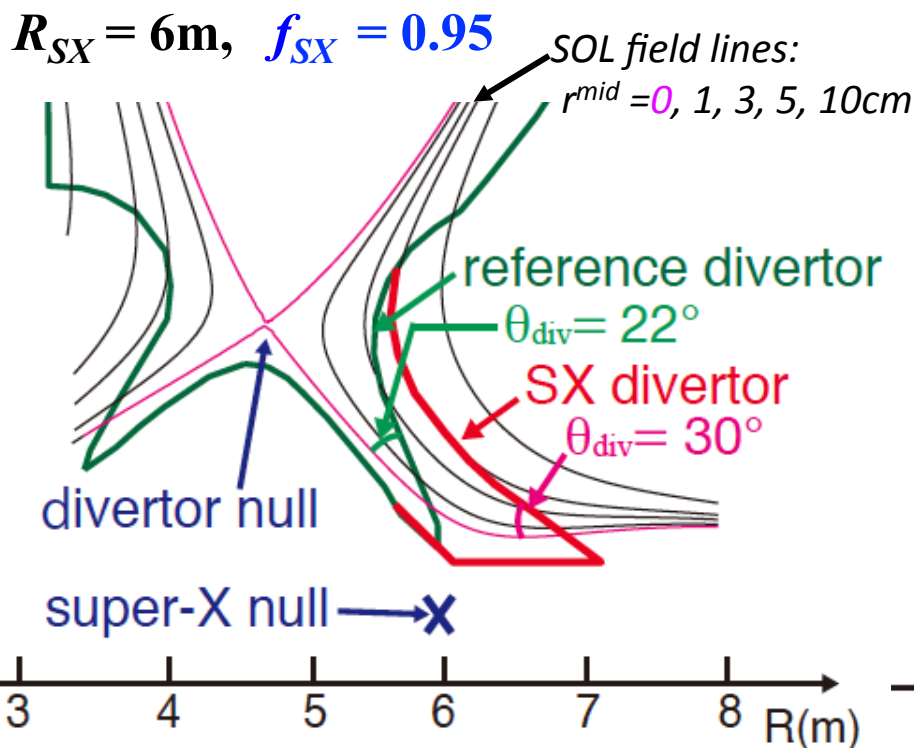
- (1) Minimum number of PFCs
- (2) PFC currents and size (inside $I_{PF} < 15\text{MA}$, 1m outside $I_{PF} < 50\text{-}60\text{MA}$, 2m)
- (3) Suitable for sector (Blanket & Divertor) replacement



Magnetic configuration for *Super-X divertor* (SXD)

Magnetic and Divertor geometries are investigated for *Super-X divertor*:

- *Flux expansion* is increased from Divertor-null to SX-null
⇒ Divertor opening becomes wider to handle SOL field lines of $r^{mid} < 5\text{cm}$.
 - *Outer target* ($R_{div} = 6.7\text{m}$) is designed *outer* the Super-X null ($R_{SX} = 6\text{m}$),
where *Target angle* (θ_{div}) is increased ⇒ further inclination of the target is required
- Effect of f_{SX} (0.95 to 0.99) on flux expansion appears near the separatrix : $< 1\text{ cm}$.*



Divertor coils and Magnetic configurations for SXD and SFD

Key divertor coils for SXD and SFD should be inside TFC, due to restriction of I_{PFC} :
 engineering issues (PFC shield, feedthrough, appropriate cassette design) should be solved.

$L_{//}$ is increased near SX- or SF-null (1.4-1.6 larger than conv. div.) for advanced divertors

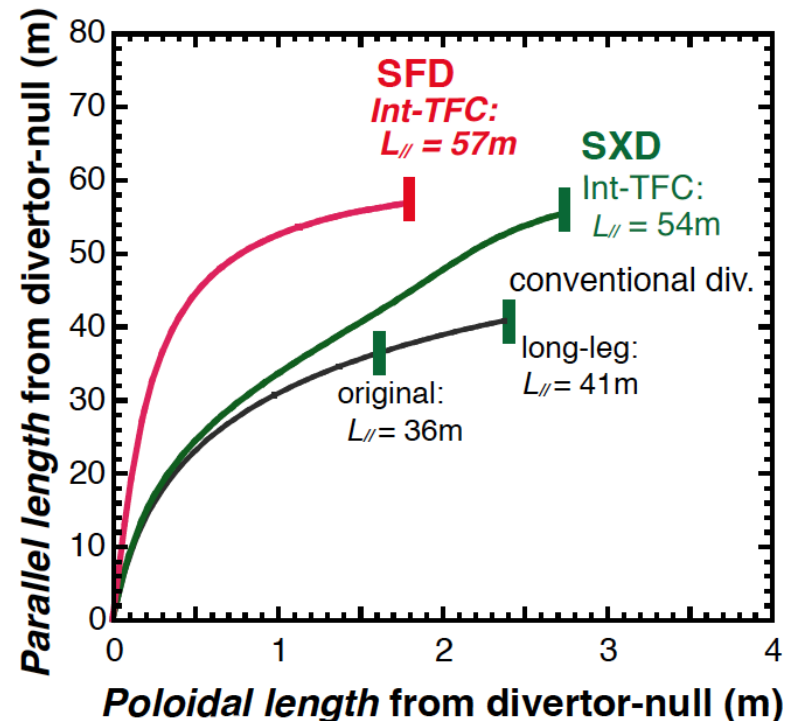
SFD: Divertor size will be compact, compared to the long-leg and SX divertors,

but f^{exp}_{div} and A_{wet} are smaller than SXD. And more ...

- Divertor geometry and the divertor coil locations are largely modified for SFD.
- Current distribution of SFD coils largely affects the lower plasma shaping.

Issues for SFD: Larger currents of the divertor and some CS coils are required, and Control scenario for the SF-null and plasma shaping must be developed.

	Conv. long-leg	SXD Int. TFC	SFD Int. TFC
PFC-7 (MA)	-2 (ext)	+10	+42
PFC-8 (MA)	+36(ext)	-4	-18
PFC-9 (MA)	+17(ext)	+18	+6
R_{div} (at target)	6.4 m	6.7m	6.2m
f^{exp}_{div} at target	2.4	3.9	2.3
Wet area, A_{wet}	1.6 m ²	1.8m ²	1.0m ²
$L_{//}$ (Xp to target)	41m	54m	57m



5. Summary and Future work for Demo power handling (1/2)

- **Enhancement of $P_{\text{rad}}^{\text{div}}$ and $P_{\text{rad}}^{\text{SOL+edge}}$ and “Full detachment”** are necessary to increase energy (plasma, radiation, neutral) dissipation in the divertor and to reduce peak q_{target} .

Seeding impurity selection: higher Z (Ar/Kr) is preferable to increase $P_{\text{rad}}^{\text{SOL}}$

- $P_{\text{rad}}^{\text{edge}}$ restriction due to confinement degradation
- dilution in core plasma

Longer leg design and divertor geometry study:

effective for full detachment and $P_{\text{rad}}^{\text{div}}$ enhancement

- reduction in ion and neutral fluxes
- appropriate size and exhaust slot location

Plasma (and impurity) diffusion – large impact on detachment and energy dissipation, suggesting that *global/local enhancement* promotes full detachment.

- database and extrapolation to Demo condition
- development of techniques

- **Conceptual design [$P_{\text{FP}}=3\text{GW}$ $P_{\text{el}}=1\text{GW}$] is now revised from many viewpoints in BA Demo Design Activity** \Rightarrow Divertor operation window will be investigated for lower P_{FP} .
- **SONIC is now improved to V3 & systematic scan in Rokkasho CSC (Helios) is planned.**
improvement/development of plasma & impurity transport modelling is necessary
 - detachment of ion flux
 - thermal force in low collisionality SOL
 - SOL flow modelling
 - coupling with edge transport (plasma&impurity), etc.

5. Summary and Future work for Advanced divertor study

“Advanced divertor” study started to provide new options of magnetic configuration. Magnetic geometry and target location were investigated **with minimal number of PFCs (9)**, using TOSCA equilibrium code.

- (1) **Super-X divertor (SXD) equilibrium** was produced by introducing 2 parameters: **SX-null location** and **Flux ratio of SX-null: $f_{SXD} = (\Psi_{SXD} - \Psi_{mag}) / (\Psi_s - \Psi_{mag})$**
 - **Connection length from divertor-null to target ($L_{//}$)** was increased compared to the conventional long-leg divertor: **1.4 - 1.9 times with f_{SXD} (0.95 to 0.99)**.
- (2) Formation of **Snowflake divertor (SFD) equilibrium** was developed:
 - **$L_{//}$ was largely increased near SF null (1.5-1.7 times)**,
⇒ SFD is compact compared to conv. and SX divertors, but key issues remain: **control scenario for SF-null and plasma shaping should be developed**, and **appropriate SFD geometry design is necessary**.
- (3) **Inter-TFC divertor coils (engineering issues)** are required both for SFD and SXD,
⇒ **appropriate design for PFC shield, feedthrough and cassette is necessary**.
coil winding and horizontal maintenance should be developed/improved.

Divertor simulation (SONIC) is developed to calculate “advanced divertor” plasma:

- **Plasma detachment and radiation distribution are investigated.**
- **Divertor geometry appropriate for detachment and pumping is determined.**

Code development:

3.1 backflow model for impurity MC calculation

MC approach for impurity transport modeling

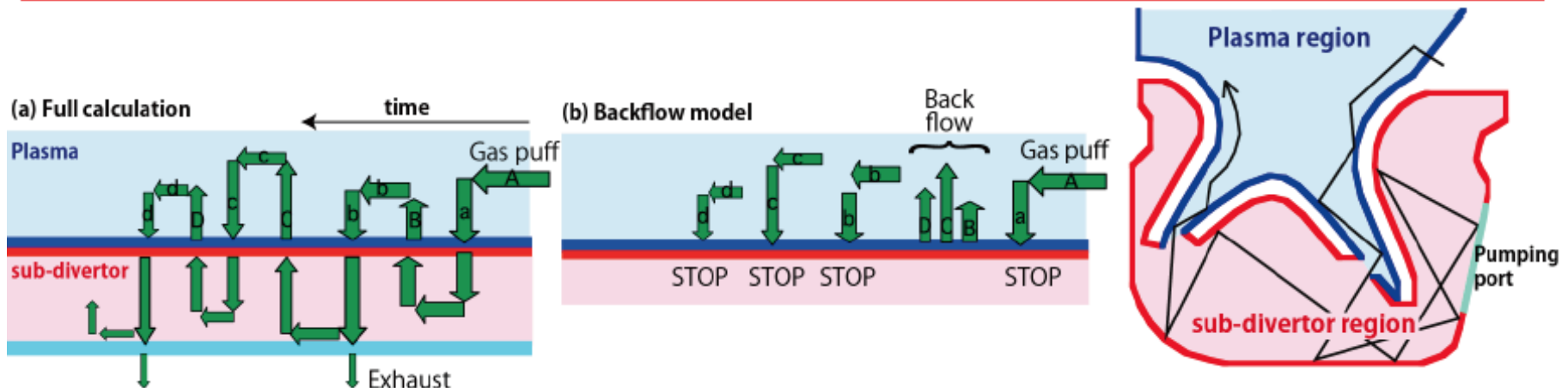
flexibility in modeling \Leftrightarrow long computational time

full calculation: trajectories of injected impurity particles are traced in the plasma and sub-divertor region.



backflow model: amount of the backflow (B, C and D) is evaluated in advance, then simulating impurity flux injected from the exhaust slot to the divertor region like a backflow.

Calculation time is reduced significantly , and iterative calculation of SONIC for DEMO divertor simulation becomes possible.



Code development: optimization on HELIOS / W transport simulation

3.2 Optimization of SONIC code on HELIOS

Calculation time and accuracy are improved by increase in computer cores.

- **wide-range parameter survey**: divertor geometry, impurity species ...
- **stable calculation** due to reduction in MC noise

BX900(JAEA) : 40 hours
128PE, 170000 MC test particles



Helios: 15 hours
1024 PE, 340000 MC test particles

Calc. time becomes **less than half** while **double** of test particles is treated.

3.3 Development of W transport simulation

Improvement of full orbit MC particle simulation code IMPGYRO is in progress to estimate lifetime of W-plasma facing components.

In the preliminary analysis with fixed background solution (partial detachment), net erosion rate was too high ($\sim 10^{-7}$ m/s) compared with the required lifetime up to next maintenance, because of large self-sputtering.

Self-consistent analysis between background and W transport is necessary.
Also influence on the core performance has to be estimated.

Development of TOSCA equilibrium code for Super-X divertor

- (1) Same location of 9 PFCs (outside TFC) is used
- (2) New input parameters for SXD are introduced,

- *Super-X null location* (R_{SX}, Z_{SX})
- *Ratio of poloidal fluxes at SX-null and separatrix:*

$$f_{SX} = (\Psi_{SX} - \Psi_{ax}) / (\Psi_s - \Psi_{ax})$$

Current distribution (I_{PFC}) is determined to minimize the following least square errors:

$$E = \sum_{k=1}^{N_s} W_k (\Psi_k - \Psi_s)^2 + \sum_{k=1}^2 \chi_k (\Psi_k - \Psi_s)^2 + \sum_{k=1}^4 \sigma_k (B_R^2 + B_Z^2) + f (\Psi_{Link} - \Psi_{Ref})^2 + \sum_{j=1}^{N_c} \gamma_j N_j^2 (I_j - I_{Ref,j})^2 + \chi_{SXD} (\Psi_{SXD} - (\Psi_{Mag} - f_{SXD} (\Psi_{Mag} - \Psi_s)))^2$$

1st & 2nd terms: Flux at selected plasma surface and null

3rd term: Mag. field at divertor & SX null points

4th term: Interlinkage flux (set to $\Psi_{Ref} = -100$ Vs)

6th term: Magnetic flux at SX-null

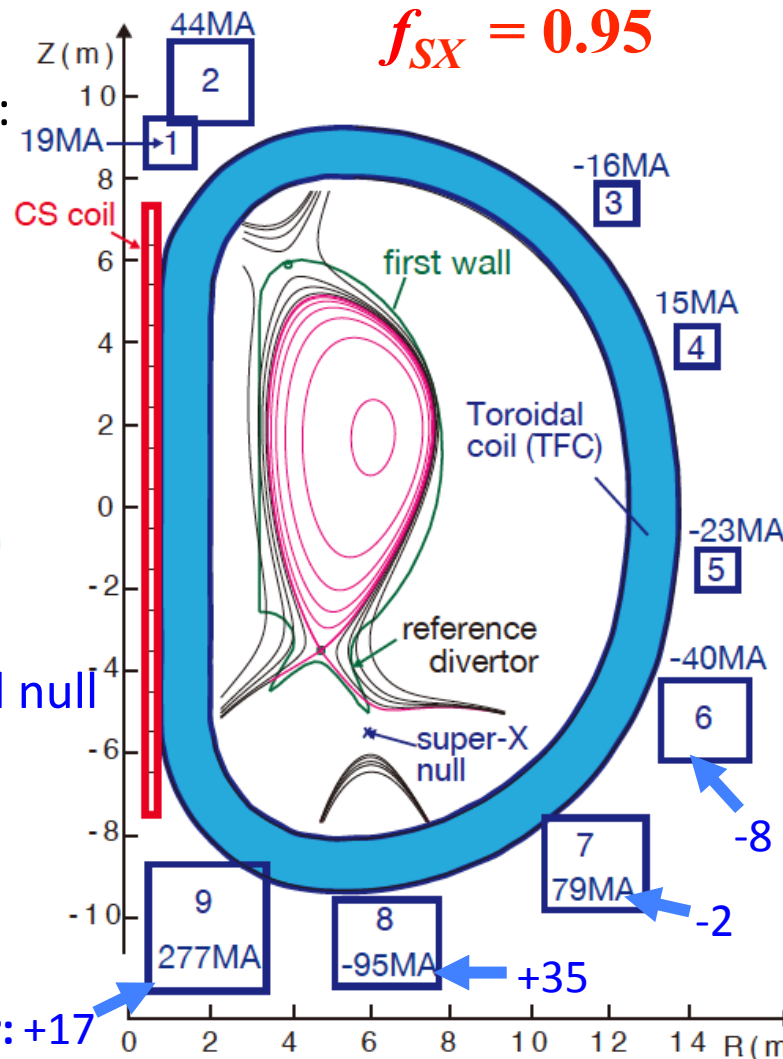
Weight factors were optimized to obtain better

accuracy of SX-null position.

I_{PFC} for Conv. Divertor: +17

$$R_{SX} = 6m$$

$$f_{SX} = 0.95$$



Note: size of PFC does not correspond to the current

Equilibrium control and divertor geometry for SFD

Equilibrium control and formation scenario of SFD have been investigated:

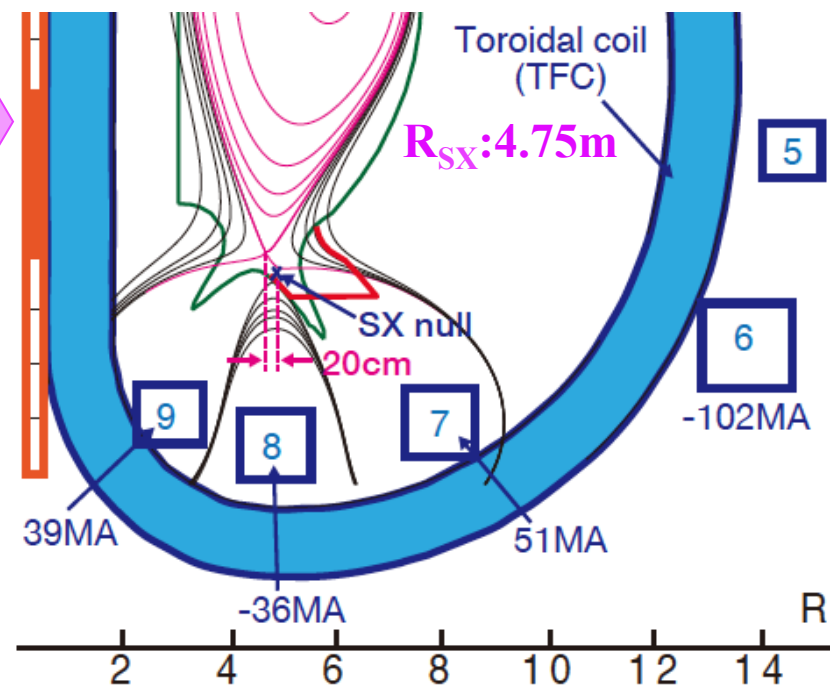
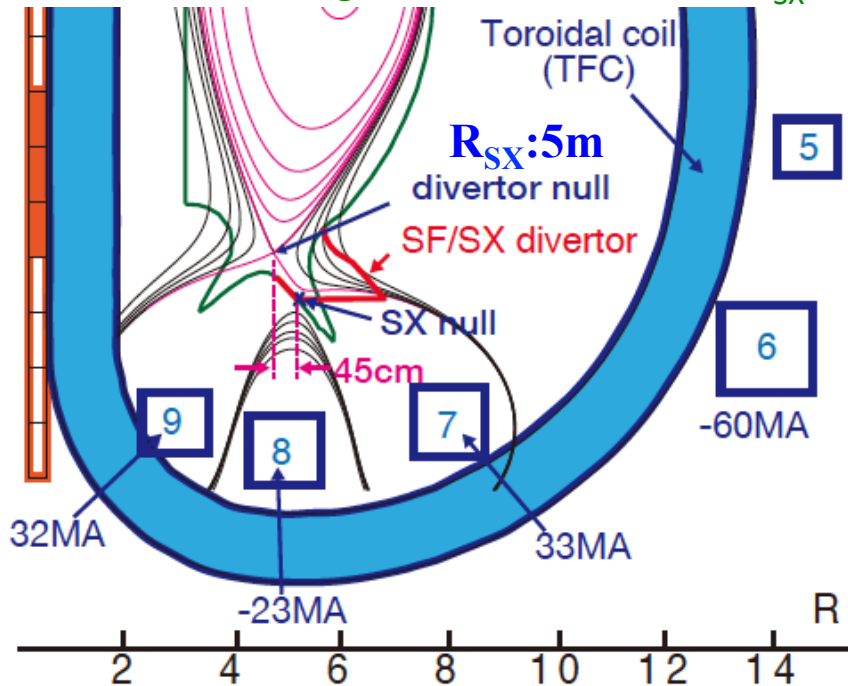
(1) from SXD to SFD with $f_{SX} \sim 0.99 (<1)$ --- below

(2) from unbalanced-SFD (SF- or SF+) to balanced-SFD --- not shown

Divertor geometry must be design for SFD&SXD, **NOT appropriate** for the conventional divertor.

Divertor coil currents must be increased to obtain balanced-SFD -> **need SFD coil arrangement.**

Divertor coil arrangement for SXD with $R_{SX}=6m$



Current (MA)	SXD $R_{SX}:6m$	SXD $R_{SX}:5m$	SXD $R_{SX}:4.75m$
PFC-7	+10	+33	+51
PFC-8	-4	-23	-36
PFC-9	+17	+32	+39

Future studies of Demo advanced divertor

[Next step for divertor physics study]

Divertor simulation (SONIC) is developed to calculate “advanced divertor” plasma:

- Plasma detachment and radiation distribution are investigated.
- Divertor geometry appropriate for detachment and pumping is determined.

[Magnetic equilibrium study]

- Divertor coil locations are optimized to reduce the PFC currents:
Combination of Inter-PFC and outer-PFC is also considered.
- PFC arrangement for horizontal replacement of sector/blanket/divertor.
- For SFD, control scenario for SF-null and plasma shaping must be developed, and unbalanced SF configurations (SF+ and SF-) are also investigated.

[Engineering issues]

- PFC design for shield and feedthrough is investigated for inter-PFC.
- Super-Conductors and Winding procedure should be determined.
- Design work of divertor geometry and target & cassette structure and both for SXD and SFD are necessary, compatible with the divertor & sector maintenance.